International Journal of Solids and Structures 254–255 (2022) 111854

Contents lists available at ScienceDirect

International Journal of Solids and Structures

journal homepage: www.elsevier.com/locate/ijsolstr

On the use of **QR** kinematics in studying the Eshelby energy–momentum tensor

Sandipan Paul [a,*], Alan D. Freed [b], László Szabó [c]

[a] Department of Civil Engineering, Indian Institute of Technology Roorkee, Roorkee, 247667, India
[b] Impact Physics Branch, U.S. Army Research Laboratory, Aberdeen Proving Ground, Aberdeen, MD 21005, United States
[c] Department of Applied Mechanics, Budapest University of Technology and Economics, H-1111 Budapest, Műegyetem rkp. 5., Hungary

ARTICLE INFO

MSC:
74A20
74C15

Keywords:
Elastic–plastic materials
Constitutive behavior
Finite strain
Variational calculus

ABSTRACT

We study the Eshelby energy–momentum tensor using **QR** kinematics, obtained from an upper-triangular decomposition of the deformation gradient. In recent years, a **QR** decomposition of the deformation gradient has gained attention because of its utility in experiments and constructing constitutive models. In this framework, the constitutive relations can be developed using scalar, conjugate, stress/strain, base pairs that have minimum couplings between them. In this paper, in addition to these scalar stress attributes, we introduce driving force attributes that are thermodynamic conjugates to the dissipative strain attributes. A one-to-one relation between the driving force attributes and the components of Eshelby's energy–momentum tensor, defined in this framework, has been established. These kinetic and kinematic quantities play a key role in the constitutive formulation of a dissipative process. Finally, a classical J_2 plasticity model has been derived to illustrate the role of these driving force attributes.

1. Introduction

Recent developments in the field of continuum mechanics, based on a **QR** decomposition of the deformation gradient, prove to be useful over the traditional methods in its various branches such as elasticity theory (Freed and Srinivasa, 2015; Freed, 2017; Erel et al., 2019; Paul and Freed, 2020b; Lembo, 2017), viscoelasticity and damage (Clayton and Freed, 2020a), plasticity (Rajagopal and Srinivasa, 2016; Paul and Freed, 2020a, 2021), rheometry (Paul et al., 2021a), mechanics of plate tectonics (Broerse et al., 2021), and biomechanics (Avazmohammadi et al., 2018; Zhang et al., 2019; Kazerooni et al., 2019; Clayton and Freed, 2020b; Zamani et al., 2021). In a **QR** decomposition, the matrix of a deformation gradient is decomposed into an orthogonal rotation matrix $\boldsymbol{\mathcal{R}}$ and an upper-triangular stretch $\boldsymbol{\mathcal{U}}$, called the Laplace stretch (Freed et al., 2019). This decomposition was first introduced into the physics literature by McLellan (1976, 1980) in his work on thermodynamic stability of crystalline phases. Srinivasa (2012) pointed out its utility over the traditional polar decomposition, as it is possible to measure the components of a Laplace stretch directly and unambiguously from experiments. Another significant advantage of this decomposition lies in its application when constructing constitutive models. Traditionally, tensor invariants are employed to derive constitutive equations whenever a polar decomposition of the deformation gradient is in use. However, Criscione (2004) showed that due to the covariance between these tensor invariants, it is difficult to parametrize a material model from an experimental standpoint. To overcome this issue, Freed et al. (2016), Freed (2017) proposed constitutive models based on scalar, conjugate, stress/strain, base pairs derived from **QR** kinematics. This decomposition was further extended to elastoplasticity by using the fact that the set of all invertible, upper-triangular matrices form a group under multiplication (Freed et al., 2019). In this work, the Laplace stretch obtained from a **QR** decomposition was factorized into its elastic and plastic components. Needless to say that both these components are upper-triangular in nature. Paul and Freed (2020a) showed that the components of plastic Laplace stretch can be measured from experiments, at least for a homogeneous rotation field. Because of these advantages and renewed interest in the application of **QR** kinematics, we venture into studying Eshelby energy–momentum tensor within this framework. Our primary motivation for this investigation is to gain some more insights about this field using the physical significance of the components of the Laplace stretch.

In his seminal works (Eshelby, 1951, 1956, 1975, 1999), Eshelby introduced the concept of an energy–momentum tensor into the mechanics literature by establishing a connection between its typical use in other field theories (e.g., Maxwell's stress tensor in electrostatics) and the force acting on a material inhomogeneity or lattice defects such as dislocations, point defects, etc. This force is often termed as

* Corresponding author.
E-mail address: sandipan.paul@ce.iitr.ac.in (S. Paul).

https://doi.org/10.1016/j.ijsolstr.2022.111854
Received 3 March 2022; Received in revised form 18 June 2022; Accepted 11 July 2022
Available online 16 July 2022

a configurational force and has been a major topic of research (Cleja-Tigoiu and Maugin, 2000; Cermelli et al., 2001; Maugin, 2016) since the introduction of Eshelby's energy–momentum tensor. The evolution of material inhomogenieties and the Eshelby stress tensor has been studied by Epstein and Maugin (1990, 1996) from a geometric point of view. Traditionally, the Eshelby energy–momentum tensor can be defined as[1]

$$\mathbf{E}^d := \psi\,\mathbf{I} - \mathbf{F}^T\,\mathbf{P}, \tag{1}$$

where $\mathbf{F}$ and $\mathbf{P}$ are the deformation gradient and first Piola–Kirchhoff stress, respectively, and ψ denotes the strain energy per unit volume in a reference configuration. This definition of the Eshelby energy–momentum tensor can be viewed as a dual of the Cauchy stress tensor (Maugin, 2016). In addition, when contracted with the velocity gradient tensor associated with a dissipative process, the Eshelby energy–momentum tensor yields the energy dissipated during the deformation process (Gupta et al., 2007). Rajagopal and Srinivasa (2005) studied the Eshelby energy–momentum tensor within the framework of Eckart's multiple natural configuration. This framework considers that a body can possess different natural configurations when it undergoes a general deformation process. The response of the body can be obtained as a family of elastic responses measured from a fixed natural configuration, whereas the evolution of these natural configurations is obtained from a thermodynamic consideration. Rajagopal and Srinivasa argued that within this framework one need not consider a separate configurational force in connection with the Eshelby energy–momentum tensor. This force appears naturally as the driving force behind any dissipative process. In the context of elastic–plastic materials, it has been shown elsewhere (Paul and Freed, 2021) that the elastic–plastic decomposition of Laplace stretch fits naturally into Eckart's multiple natural configuration framework. Therefore, in this paper, we study the Eshelby energy–momentum tensor using an upper-triangular decomposition of the deformation gradient within this framework. Although the concept of Eshelby's energy–momentum tensor has been used to study other problems in mechanics such as inclusions, crack initiation and propagation in fracture mechanics etc., here we confine our attention to problems involving a multiplicative decomposition of the deformation gradient. This paper is primarily focused on the theoretical development; applications of the proposed theory will be addressed in subsequent works.

The rest of the paper is organized as follows. In Section 2, we briefly review the **QR** kinematics and relevant kinetic quantities and their physical significance. The concept of natural configurations in this context is also revisited in Section 2.3. We introduce the driving force attributes following Eshelby's method in Section 3.1. The driving force attributes are scalar alternatives of the Eshelby energy–momentum tensor and correspond to the concept of configurational forces. To demonstrate that, we first derive an equivalent definition for the Eshelby energy–momentum tensor, $\boldsymbol{\mathcal{E}}$ within our framework in Section 3.2. A one-to-one map can be established between the components of $\boldsymbol{\mathcal{E}}$ and the driving force attributes. This map changes slightly when the material exhibits an evolving anisotropy throughout the dissipative process as shown in Section 3.3. The role of the driving force attributes in the constitutive formulation has been studied in Section 4. An illustration of the classical J_2 plasticity has been worked out in this framework in Section 4.1. Finally, the paper is summarized and drawn to conclusions.

[1] In the literature, the Eshelby energy–momentum tensor has also been defined as $\mathbf{E}^d := \mathbf{F}^T\,\mathbf{P} - \psi\,\mathbf{I}$ (cf. Epstein and Maugin (1990, § 3, Eq. (12))) which is negative of the one defined in Epstein and Maugin (1996, § 4, Eq. (28)) and, Gupta et al. (2007, § 3, Eq. (35)). The sign in the definition of the Eshelby energy–momentum tensor is of little consequence as long as it is consistent with the calculation of the energy dissipated during a thermodynamic process. In fact, the definition of an energy–momentum tensor is also dependent on the definition of the associated velocity gradient.

2. Preliminaries

2.1. Laplace stretch and modes of deformation

Let us consider a body $\mathcal{B}$ with a typical material particle $\mathcal{P}$ in it. Let $\kappa_r(\mathcal{B})$ and $\kappa_t(\mathcal{B})$ denote the reference and current configurations of the body respectively. The deformation gradient $\mathbf{F}$ takes an infinitesimal fiber dX from the tangent space of $\kappa_r(\mathcal{B})$ and places it into the current configuration $\kappa_t(\mathcal{B})$ which is denoted by dx. If $x(X,t)$ denotes the deformation map of the body, then the deformation gradient can be written as

$$\mathbf{F} = \frac{\partial x(X,t)}{\partial X}. \tag{2}$$

When expressed in a coordinate system, the matrix representation of the deformation gradient turns out to be a full matrix. The matrix of the deformation gradient is re-indexed according to the strategy proposed by Paul et al. (2021b) in order to avoid any ambiguity regarding the representation of the Laplace stretch, which plays a key role in our subsequent analysis. This strategy is particularly useful in the case of isotropy, as an isotropic material does not inherently have any preferred coordinate direction. With an increase in anisotropy of a material, the proposed strategy becomes simpler, i.e., it involves fewer possible coordinate permutations via orthogonal rotation tensors, used in re-indexing. For an anisotropic material, the deformation gradient can be directly used without employing any re-indexing strategy. A set of suitable coordinate directions must be chosen in that case.

Now we perform a **QR** decomposition on the re-indexed deformation gradient by using a Gram–Schmidt procedure. In this method, a new set of bases $\{\tilde{\boldsymbol{e}}_i\}$ is obtained by employing Laplace's successive orthogonal projections on the columns of the re-indexed deformation gradient, $\boldsymbol{f}_i$. These bases can be written as

$$\begin{aligned}
\tilde{\boldsymbol{e}}_1 &= \frac{\boldsymbol{f}_1}{\|\boldsymbol{f}_1\|};\\
\tilde{\boldsymbol{e}}_2 &= \frac{\boldsymbol{f}_2 - (\boldsymbol{f}_1\cdot\boldsymbol{f}_2)\,\boldsymbol{f}_1}{\|\boldsymbol{f}_2 - (\boldsymbol{f}_1\cdot\boldsymbol{f}_2)\,\boldsymbol{f}_1\|};\\
\tilde{\boldsymbol{e}}_3 &= \frac{\boldsymbol{f}_3 - (\boldsymbol{f}_1\cdot\boldsymbol{f}_3)\,\boldsymbol{f}_1 - (\boldsymbol{f}_2\cdot\boldsymbol{f}_3)\,\boldsymbol{f}_2}{\|\boldsymbol{f}_3 - (\boldsymbol{f}_1\cdot\boldsymbol{f}_3)\,\boldsymbol{f}_1 - (\boldsymbol{f}_2\cdot\boldsymbol{f}_3)\,\boldsymbol{f}_2\|}.
\end{aligned} \tag{3}$$

The resultant decomposition is given as

$$\boldsymbol{\mathcal{F}} = \boldsymbol{\mathcal{R}}\,\boldsymbol{\mathcal{U}} \tag{4a}$$

where

$$[\mathcal{R}_{ij}] = \left[\tilde{\boldsymbol{e}}_1 \mid \tilde{\boldsymbol{e}}_2 \mid \tilde{\boldsymbol{e}}_3\right] \text{ and } [\mathcal{U}_{ij}] = \begin{bmatrix} a & a\gamma & a\beta \\ 0 & b & b\alpha \\ 0 & 0 & c \end{bmatrix}. \tag{4b}$$

Note that here we have adopted a Lagrangian description. In an Eulerian description, the bases $\{\tilde{\boldsymbol{e}}_i\}$ are obtained by using the same method on the rows of the re-indexed deformation gradient. In addition, the resulting Laplace stretch is lower-triangular in nature (Freed et al., 2020). The above decomposition is starkly different from a traditional polar decomposition, $\mathbf{F} = \mathbf{R}\,\mathbf{U}$ where $\mathbf{U}$ is a symmetric stretch tensor, and the rotation $\mathbf{R}$ is different from $\boldsymbol{\mathcal{R}}$.

The Laplace stretch can be further decomposed into two shearing motions followed by an extensional motion along the three coordinate directions $\{\tilde{\boldsymbol{e}}_i\}$ (Srinivasa, 2012), resulting in an Iwasawa decomposition (Iwasawa, 1949). This decomposition can be written as

$$[\mathcal{U}_{ij}] = \underbrace{\begin{bmatrix} a & 0 & 0 \\ 0 & b & 0 \\ 0 & 0 & c \end{bmatrix}}_{\Lambda} \underbrace{\begin{bmatrix} 1 & 0 & \beta \\ 0 & 1 & \alpha \\ 0 & 0 & 1 \end{bmatrix}}_{\mathcal{U}^{\alpha\beta}} \underbrace{\begin{bmatrix} 1 & \gamma & 0 \\ 0 & 1 & 0 \\ 0 & 0 & 1 \end{bmatrix}}_{\mathcal{U}^{\gamma}}. \tag{5}$$

In order to identify the different modes of deformation, the extensional motion $\boldsymbol{\Lambda}$ was further decomposed as

$$[\Lambda_{ij}] = \underbrace{\sqrt[3]{abc}\begin{bmatrix}1&0&0\\0&1&0\\0&0&1\end{bmatrix}}_{\text{dilatation}} \times \underbrace{\begin{bmatrix}\sqrt[3]{a/b}&0&0\\0&\sqrt[3]{b/a}&0\\0&0&1\end{bmatrix}}_{\text{1-2 planar squeeze}} \times \underbrace{\begin{bmatrix}1&0&0\\0&\sqrt[3]{b/c}&0\\0&0&\sqrt[3]{c/b}\end{bmatrix}}_{\text{2-3 planar squeeze}} \times \underbrace{\begin{bmatrix}\sqrt[3]{a/c}&0&0\\0&1&0\\0&0&\sqrt[3]{c/a}\end{bmatrix}}_{\text{3-1 planar squeeze}}. \tag{6}$$

Therefore, the Laplace stretch is decomposed into seven modes of deformation: one dilatation, three squeezes, and three shears. Based on these modes of deformation, one can deconstruct the stress power in terms of scalar, conjugate, stress/strain, base pairs.

2.2. Conjugate stress/strain base pairs

Let **P**, **S** and **E** denote the first and second Piola–Kirchhoff stresses and the Green strain, respectively. The stress power at a material point can be written as

$$\dot{W} := \mathrm{tr}(\mathbf{P}^T\,\dot{\mathbf{F}}) = \mathrm{tr}(\mathbf{S}\,\dot{\mathbf{E}}) = \mathrm{tr}(\boldsymbol{\mathcal{S}}\,\boldsymbol{\mathcal{L}}) \tag{7}$$

where $\boldsymbol{\mathcal{L}}$ is a velocity gradient defined as $\boldsymbol{\mathcal{L}} := \dot{\boldsymbol{\mathcal{U}}}\,\boldsymbol{\mathcal{U}}^{-1}$ and $\boldsymbol{\mathcal{S}}$ is the Kirchhoff stress in our physical frame of reference. The Kirchhoff stress $\boldsymbol{\mathcal{S}}$ is related to **S** through $\boldsymbol{\mathcal{S}} := \boldsymbol{\mathcal{U}}\,\mathbf{S}\,\boldsymbol{\mathcal{U}}^T$ and is symmetric because of the symmetry of the second Piola–Kirchhoff stress.

Now, in accordance with Eqs. (5) and (6), we can define strain attributes corresponding to each mode of deformation. Let δ, ε_i and γ_i denote the strain attributes corresponding to the modes of dilatation, squeeze and shear, respectively. These strain attributes and their rates are defined as

$$\delta := \tfrac{1}{3}\ln(abc), \quad \dot{\delta} = \frac{1}{3}\left(\frac{\dot{a}}{a} + \frac{\dot{b}}{b} + \frac{\dot{c}}{c}\right); \tag{8a}$$

$$\varepsilon_1 := \tfrac{1}{3}\ln(a/b), \quad \dot{\varepsilon_1} = \frac{1}{3}\left(\frac{\dot{a}}{a} - \frac{\dot{b}}{b}\right); \tag{8b}$$

$$\varepsilon_2 := \tfrac{1}{3}\ln(b/c), \quad \dot{\varepsilon_2} = \frac{1}{3}\left(\frac{\dot{b}}{b} - \frac{\dot{c}}{c}\right); \tag{8c}$$

$$\varepsilon_3 := \tfrac{1}{3}\ln(c/a), \quad \dot{\varepsilon_3} = \frac{1}{3}\left(\frac{\dot{c}}{c} - \frac{\dot{a}}{a}\right); \tag{8d}$$

$$\gamma_1 := \alpha; \quad \dot{\gamma}_1 = \dot{\alpha}; \tag{8e}$$

$$\gamma_2 := \beta; \quad \dot{\gamma}_2 = \dot{\beta}; \tag{8f}$$

$$\gamma_3 := \gamma; \quad \dot{\gamma}_3 = \dot{\gamma}. \tag{8g}$$

From Eqs. (8b), (8c) and (8d), it is evident that one of the squeeze strain (or strain rate) attributes can be expressed as a linear combination of the other two. This is a manifestation of the fact that not all squeeze modes are independent of each other. It is possible to establish a one-to-one map between the strain rate attributes and the components of the velocity gradient $\boldsymbol{\mathcal{L}}$. This map, however, is not unique and depends on the material behavior. In particular, an anisotropic material behavior is modeled in our framework by introducing anisotropy parameters in the map between the strain rate attributes and components of $\boldsymbol{\mathcal{L}}$. If π, σ_i and τ_i denote the thermodynamic conjugates (stress attributes) to the strain attributes corresponding to dilatation, squeeze and shear, respectively, then these stress attributes can be obtained as

$$\pi := \mathcal{S}_{11} + \mathcal{S}_{22} + \mathcal{S}_{33}; \tag{9a}$$

$$\sigma_1 := \mathcal{S}_{11} - \mathcal{S}_{22}; \tag{9b}$$

$$\sigma_2 := \mathcal{S}_{22} - \mathcal{S}_{33}; \tag{9c}$$

$$\sigma_3 := \mathcal{S}_{33} - \mathcal{S}_{11}; \tag{9d}$$

$$\tau_1 := b/c\;\mathcal{S}_{23}; \tag{9e}$$

$$\tau_2 := a/c\;\mathcal{S}_{13}; \tag{9f}$$

$$\tau_3 := a/b\;\mathcal{S}_{12} - \alpha a/c\;\mathcal{S}_{13}. \tag{9g}$$

Eqs. (9e), (9f) and (9g) manifest that a coupling exists between the squeeze and shear modes of deformation.

The stress power can now be written in terms of the stress and strain rate attributes as

$$\dot{W} = \pi\,\dot{\delta} + \sum_{i=1}^{3}(\sigma_i\,\dot{\varepsilon}_i + \tau_i\,\dot{\gamma}_i). \tag{10}$$

2.3. Natural configurations and decomposition of Laplace stretch into dissipative and elastic parts

When a body is mechanically loaded, it can undergo two types of thermodynamic processes: (i) the body dissipates energy, i.e., converts mechanical energy into heat and, (ii) it stores the mechanical energy and releases it to get back to its original configuration upon unloading. The latter is often termed as an elastic deformation process, whereas the former process goes by different names based upon the material behaviors under consideration. Here we call the former process as a dissipative process in order to cover a broad range of processes that a body can undergo (e.g., elastoplasticity Lee, 1969, thermoelasticity Lubarda, 2004, growth mechanics in soft elastic tissues Rodriguez et al., 1994, etc.). For a general deformation of the body, these processes can be described within the framework of Eckart's multiple natural configurations. In this framework, it is considered that a body can possess multiple natural configurations which evolve through a dissipative process. Thus, the overall response of the body can be obtained as a family of elastic responses measured from a fixed natural configuration.

At this juncture, it is important to understand the physical significance of **QR** kinematics. Fig. 1 demonstrates all the necessary configurations and transformations relevant to our framework. As mentioned earlier, the deformation gradient takes an infinitesimal fiber from the reference configuration of the body $\kappa_r(\mathcal{B})$ and places it into its current configuration $\kappa_t(\mathcal{B})$. The inverse to the rotation tensor $\boldsymbol{\mathcal{R}}^T$ takes the infinitesimal fiber from $\kappa_t(\mathcal{B})$ into our physical frame of reference in which the bases $\{\tilde{\boldsymbol{e}}_i\}$ are obtained from a Gram–Schmidt procedure. This physical frame of reference is denoted by $\tilde{\kappa}_t(\mathcal{B})$. The configurations $\kappa_r(\mathcal{B})$ and $\tilde{\kappa}_t(\mathcal{B})$ are related through the Laplace stretch $\boldsymbol{\mathcal{U}}$. Thus, the rotation $\boldsymbol{\mathcal{R}}$ takes an important role in coordinate transformation, whereas the deformation of a body in all six degrees of freedom is completely described by the components of Laplace stretch.

Following Freed et al. (2019), the Laplace stretch is now further decomposed into two upper-triangular matrices corresponding to a dissipative ($\boldsymbol{\mathcal{U}}^d$) and an elastic ($\boldsymbol{\mathcal{U}}^e$) deformation process. This decomposition is written as

$$\boldsymbol{\mathcal{U}} = \boldsymbol{\mathcal{U}}^e\,\boldsymbol{\mathcal{U}}^d \tag{11a}$$

where

$$[\mathcal{U}^e_{ij}] = \begin{bmatrix}a^e & a^e\gamma^e & a^e\beta^e\\0 & b^e & b^e\alpha^e\\0&0&c^e\end{bmatrix} \quad \text{and} \quad [\mathcal{U}^d_{ij}] = \begin{bmatrix}a^d & a^d\gamma^d & a^d\beta^d\\0 & b^d & b^d\alpha^d\\0&0&c^d\end{bmatrix}. \tag{11b}$$

Components of the elastic and dissipative parts of Laplace stretch have the same physical meanings as those of the total Laplace stretch. The

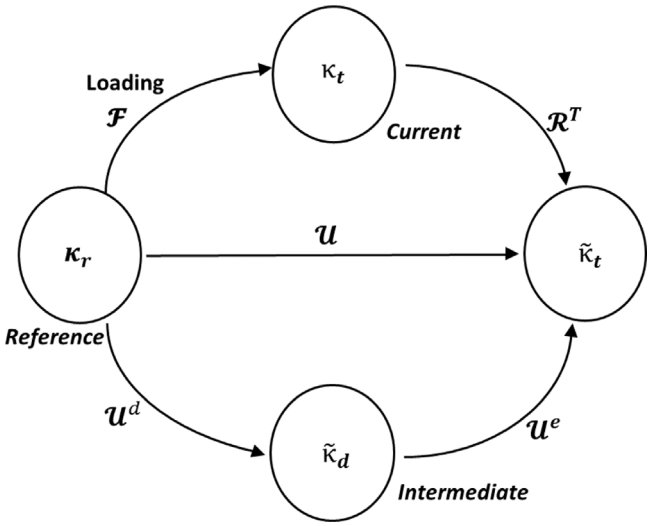

Fig. 1. Different configurations associated with **QR** kinematics and related transformations. The deformation gradient **F** takes an infinitesimal fiber from the reference configuration $\kappa_r(\mathcal{B})$ to the current configuration $\kappa_t(\mathcal{B})$. The inverse to the rotation tensor $\boldsymbol{\mathcal{R}}^T$ takes this infinitesimal fiber into our physical frame of reference $\tilde{\kappa}_t(\mathcal{B})$. $\tilde{\kappa}_t$ is thus related to the reference configuration through the Laplace stretch. In view of the decomposition of the Laplace stretch, we introduce an intermediate configuration $\tilde{\kappa}_d$ that is related to the reference configuration through the dissipative part of Laplace stretch $\mathcal{U}^d$. The elastic part of Laplace stretch takes an infinitesimal fiber from this configuration to the configuration κ_d. Note that one can reach configuration κ_d either by employing the total Laplace stretch $\mathcal{U}$ or from the current configuration κ_t through a change of bases. These two procedures have different physical interpretations. Nevertheless, the resultant configuration is the same, and thus, is denoted interchangeably by κ_d or $\tilde{\kappa}_t$.

components of Laplace stretch, and its elastic and dissipative parts, are related through

$$\begin{aligned} a &= a^e a^d, \quad \alpha = c^d \alpha^e / b^d + \alpha^d, \\ b &= b^e b^d, \quad \beta = c^d \beta^e / a^d + b^d \gamma^e \alpha^d / a^d + \beta^d, \\ c &= c^e c^d, \quad \gamma = b^d \gamma^e / a^d + \gamma^d. \end{aligned} \tag{12}$$

The decomposition in Eq. (11) induces another intermediate, configuration $\tilde{\kappa}_d(\mathcal{B})$ that is related to the reference configuration $\kappa_r(\mathcal{B})$ and the configuration $\tilde{\kappa}_t(\mathcal{B})$ through the dissipative and elastic parts of Laplace stretch, respectively. Clearly, the configuration $\tilde{\kappa}_d(\mathcal{B})$ acts as a natural configuration in the terminology of Eckart. If $\boldsymbol{\mathcal{L}}^d := \dot{\boldsymbol{\mathcal{U}}}^d \boldsymbol{\mathcal{U}}^{d^{-1}}$ is the velocity gradient corresponding to the dissipative process, then the evolution equation for $\boldsymbol{\mathcal{L}}^d$ governs the evolution of the configuration $\tilde{\kappa}_d(\mathcal{B})$.

Following Eqs. (8a)–(8g), one can define the elastic and dissipative strain attributes as

$$\begin{aligned} \delta^e = \tfrac{1}{3}\ln(a^e b^e c^e), \quad \varepsilon_1^e = \tfrac{1}{3}\ln(a^e/b^e), \quad \varepsilon_2^e = \tfrac{1}{3}\ln(b^e/c^e), \\ \varepsilon_3^e = \tfrac{1}{3}\ln(c^e/a^e), \\ \gamma_1^e = \alpha^e, \quad \gamma_2^e = \beta^e, \quad \gamma_3^e = \gamma^e \end{aligned} \tag{13a}$$

and

$$\begin{aligned} \delta^d = \tfrac{1}{3}\ln(a^d b^d c^d), \quad \varepsilon_1^d = \tfrac{1}{3}\ln(a^d/b^d), \quad \varepsilon_2^d = \tfrac{1}{3}\ln(b^d/c^d), \\ \varepsilon_3^d = \tfrac{1}{3}\ln(c^d/a^d), \\ \gamma_1^d = \alpha^d, \quad \gamma_2^d = \beta^d, \quad \gamma_3^d = \gamma^d \end{aligned} \tag{13b}$$

where the superscripts '$\square^e$' and '$\square^d$' correspond to an elastic and a dissipative process respectively. The total strain attributes and its elastic and dissipative parts are related via

$$\begin{aligned} &\delta = \delta^e + \delta^d, \\ &\varepsilon_i = \varepsilon_i^e + \varepsilon_i^d \ (i = 1, 2, 3), \\ &\gamma_1 = \exp(-3\varepsilon_1^d)\,\gamma_1^e + \gamma_1^d, \\ &\gamma_2 = \exp(3\varepsilon_3^d)\,\gamma_2^e + \gamma_2^d + \gamma_1^d\,(\gamma_3 - \gamma_3^d), \\ &\gamma_3 = \exp(-3\varepsilon_1^d)\,\gamma_3^d + \gamma_3^d. \end{aligned} \tag{14}$$

As in the case of total Laplace stretch, there exists a one-to-one correspondence between the strain rate attributes corresponding to the dissipative process and the components of $\boldsymbol{\mathcal{L}}^d$. However, this relation depends on the isotropy of the material. For the sake of simplicity, we assume that the material remains isotropic throughout the deformation process for the time being. The dissipative strain rate attributes can be obtained from the components of $\boldsymbol{\mathcal{L}}^d$ by using

$$\begin{Bmatrix} \dot{\delta}^d \\ \dot{\varepsilon}_1^d \\ \dot{\varepsilon}_2^d \\ \dot{\gamma}_1^d \\ \dot{\gamma}_2^d \\ \dot{\gamma}_3^d \end{Bmatrix} = \begin{bmatrix} 1/3 & 1/3 & 1/3 & 0 & 0 & 0 \\ 1/3 & -1/3 & 0 & 0 & 0 & 0 \\ 0 & 1/3 & -1/3 & 0 & 0 & 0 \\ 0 & 0 & 0 & c^d/b^d & 0 & 0 \\ 0 & 0 & 0 & 0 & c^d/a^d & b^d\alpha^d/a^d \\ 0 & 0 & 0 & 0 & 0 & b^d/a^d \end{bmatrix} \begin{Bmatrix} \mathcal{L}_{11}^d \\ \mathcal{L}_{22}^d \\ \mathcal{L}_{33}^d \\ \mathcal{L}_{23}^d \\ \mathcal{L}_{13}^d \\ \mathcal{L}_{12}^d \end{Bmatrix}. \tag{15}$$

For convenience in notation, let us define the following lists of variables.

Strain attributes:

$$l_{\mathcal{U}} := \{\delta \quad \varepsilon_1 \quad \varepsilon_2 \quad \varepsilon_3 \quad \gamma_1 \quad \gamma_2 \quad \gamma_3\}\,, \tag{16a}$$

$$l_{\mathcal{U}^d} := \{\delta^d \quad \varepsilon_1^d \quad \varepsilon_2^d \quad \varepsilon_3^d \quad \gamma_1^d \quad \gamma_2^d \quad \gamma_3^d\}\,, \tag{16b}$$

$$l_{\mathcal{U}^e} := \{\delta^e \quad \varepsilon_1^e \quad \varepsilon_2^e \quad \varepsilon_3^e \quad \gamma_1^e \quad \gamma_2^e \quad \gamma_3^e\}\,, \tag{16c}$$

Strain rate attributes:

$$l_{\dot{\mathcal{U}}} := \{\dot{\delta} \quad \dot{\varepsilon}_1 \quad \dot{\varepsilon}_2 \quad \dot{\varepsilon}_3 \quad \dot{\gamma}_1 \quad \dot{\gamma}_2 \quad \dot{\gamma}_3\}\,, \tag{16d}$$

$$l_{\dot{\mathcal{U}}^d} := \{\dot{\delta}^d \quad \dot{\varepsilon}_1^d \quad \dot{\varepsilon}_2^d \quad \dot{\varepsilon}_3^d \quad \dot{\gamma}_1^d \quad \dot{\gamma}_2^d \quad \dot{\gamma}_3^d\}\,, \tag{16e}$$

$$l_{\dot{\mathcal{U}}^e} := \{\dot{\delta}^e \quad \dot{\varepsilon}_1^e \quad \dot{\varepsilon}_2^e \quad \dot{\varepsilon}_3^e \quad \dot{\gamma}_1^e \quad \dot{\gamma}_2^e \quad \dot{\gamma}_3^e\}\,, \tag{16f}$$

Stress attributes:

$$l_{\sigma} := \{\pi \quad \sigma_1 \quad \sigma_2 \quad \sigma_3 \quad \tau_1 \quad \tau_2 \quad \tau_3\}\,. \tag{16g}$$

These definitions complete the kinematic preliminaries required for our subsequent derivations.

3. The Eshelby energy–momentum tensor and driving force attributes

To describe the response of a body within our multiple natural-configurations framework, we need to specify constitutive assumptions for two thermodynamic quantities: (i) a stress potential associated with the elastic process and, (ii) a rate of dissipation function per unit volume, ξ. Here we assume that the body undergoes only isothermal process so that the stress potential is the same as a Helmholtz potential, ψ. The isothermal version of the energy balance equation stipulates that the rate of dissipation function can be written as the difference between the mechanical power and the rate of change of the Helmholtz potential, i.e.,

$$\xi := \dot{W} - \rho_0\,\dot{\psi} \geq 0. \tag{17}$$

The non-negativity of ξ ensures that some version of the second law of thermodynamics, such as a Clausius–Duhem inequality, is identically satisfied (Rajagopal and Srinivasa, 2004). Note that the second part of Eq. (17) denotes an energy release rate. Thus, a tacit assumption in Eq. (17) is that the energy released is completely dissipated through various mechanisms, depending upon the thermodynamic process under consideration. These mechanisms include movement of

dislocations in case of plastic deformation in metals, network scission and reformation in polymers, etc.

Now we choose functional forms for the Helmholtz potential ψ and the rate of dissipation function ξ based upon the thermodynamic processes. Because the Helmholtz potential is associated with an elastic response of a body measured from a fixed natural configuration, it is reasonable to assume that it depends on the elastic strain attributes, $l_{\mathcal{U}^e}$ alone. The elastic strain attributes, in turn, can be expressed in terms of the total strain attributes and the dissipative strain attributes according to Eq. (14). Therefore, the Helmholtz potential function is considered to have a functional form of

$$\psi = \overline{\psi}(\boldsymbol{\mathcal{U}}, \boldsymbol{\mathcal{U}}^d) = \hat{\psi}(l_{\mathcal{U}}, l_{\mathcal{U}^d}). \tag{18}$$

On the other hand, the rate of dissipation function ξ determines an evolution of the natural configuration $\bar{\kappa}_d$. Therefore, this rate of dissipation function is assumed to depend upon the dissipative strain attributes and their rates. Thus, the dissipation function can be written as

$$\xi = \overline{\xi}(\boldsymbol{\mathcal{U}}^d, \boldsymbol{\mathcal{L}}^d) = \hat{\xi}(l_{\mathcal{U}^d}, l_{\dot{\mathcal{U}}^d}). \tag{19}$$

Note that for an elastic process, the dissipative strain rate attributes are zero, i.e., $l_{\dot{\mathcal{U}}^d} = \mathbf{0}$. Because an elastic process is non-dissipative, we therefore stipulate that

$$\xi = \hat{\xi}(l_{\mathcal{U}^d}, \mathbf{0}) = 0. \tag{20}$$

3.1. Driving force attributes

Now we use the method proposed by Eshelby (1956, 1975) to derive the driving forces behind a dissipative process (e.g., forces acting on a dislocation) corresponding to each mode of deformation. Since the Helmholtz potential ψ gives us the stored energy per unit volume, the total stored energy Ψ during an elastic process is given by

$$\Psi = \int_V \rho_0 \psi \, dV = \int_V \rho_0 \, \hat{\psi}(l_{\mathcal{U}}, l_{\mathcal{U}^d}) \, dV. \tag{21}$$

Let us consider a small virtual displacement $\bar{l}_{\mathcal{U}^d}$ imposed while holding constant the total and dissipative strain attributes, $l_{\mathcal{U}}$ and $l_{\mathcal{U}^d}$, respectively. The total elastic energy in this setting is given as

$$\Psi = \int_V \rho_0 \, \hat{\psi}(l_{\mathcal{U}}, l_{\mathcal{U}^d} + \alpha \, \bar{l}_{\mathcal{U}^d}) \, dV \tag{22}$$

where α is a sufficiently small parameter. The driving force behind a dissipative process is obtained from the total stored energy Ψ such that its inner product with the dissipative strain attributes result in the total stored energy in Eq. (22). From Eq. (22), we arrive at

$$-\left.\frac{\partial \Psi}{\partial \alpha}\right|_{\alpha=0} = -\int_V \rho_0 \left[\frac{\partial \psi}{\partial \delta^d} \, \overline{\delta}^d + \sum_{i=1}^{3} \left(\frac{\partial \psi}{\partial \varepsilon_i^d} \, \overline{\varepsilon}_i^d + \frac{\partial \psi}{\partial \gamma_i^d} \, \overline{\gamma}_i^d \right) \right] dV. \tag{23}$$

Now let us define a list of variables l_{σ^d} such that

$$l_{\sigma^d} = \{ \pi^d \mid \sigma_1^d \mid \sigma_2^d \mid \sigma_3^d \mid \tau_1^d \mid \tau_2^d \mid \tau_3^d \} \tag{24a}$$

where

$$\pi^d = -\rho_0 \frac{\partial \psi}{\partial \delta^d}; \quad \sigma_i^d = -\rho_0 \frac{\partial \psi}{\partial \varepsilon_i^d}; \quad \tau_i^d = -\rho_0 \frac{\partial \psi}{\partial \gamma_i^d}, \quad i = 1, 2, 3. \tag{24b}$$

Because Eq. (22) is valid for any arbitrary volume, one can assume that the associated energy can be expressed as an inner product between l_{σ^d} and $l_{\mathcal{U}^d}$. Note that Eq. (24b) essentially serves as a constitutive relation under this assumption. The variables listed in l_{σ^d} denote the configurational forces corresponding to dilatation, squeeze and shear modes of deformation, respectively, in the terminology of Eshelby and others. We call the variables listed in l_{σ^d} "driving force attributes". The derived driving force attributes have two primary advantages: (i) instead of second-order tensors, one can deal with scalar quantities that, in turn, help in simplifying analytical calculations, significantly, and to also save computational cost when performing numerical simulations and, (ii) it gives us more insight into the notion of configurational forces, as one can directly identify the components corresponding to a particular mode of deformation. The physical meanings of the driving force attributes are discussed next.

3.2. Relation between driving force attributes and Eshelby's energy–momentum tensor

To understand the physical meanings of the driving force attributes, let us first derive an equivalent definition for the Eshelby energy–momentum tensor in our framework. For the time being, we work with tensor-valued quantities such as the Laplace stretch $\boldsymbol{\mathcal{U}}$, instead of their corresponding scalar attributes, e.g., those listed in $l_{\mathcal{U}}$. Let us consider a strain–energy function $\overline{\psi}(\boldsymbol{\mathcal{U}}^e)$ per unit volume for a reference configuration $\kappa_r(\mathcal{B})$ of a body. This function describes the elastic deformation of a body for a fixed natural configuration. We further assume that this strain–energy function is related to the total Laplace stretch and its dissipative part only through the elastic Laplace stretch $\boldsymbol{\mathcal{U}}^e$. Therefore, we can write

$$\hat{\psi}(\boldsymbol{\mathcal{U}}, \boldsymbol{\mathcal{U}}^d) = J_{\mathcal{U}^d} \, \overline{\psi}(\boldsymbol{\mathcal{U}}^e) \tag{25}$$

where $J_{\mathcal{U}^d} := \det(\boldsymbol{\mathcal{U}}^d)$ is the Jacobian of the deformation between the configurations $\kappa_r(\mathcal{B})$ and $\bar{\kappa}_d(\mathcal{B})$. A time-derivative of Eq. (25) yields

$$\dot{\hat{\psi}} = J_{\mathcal{U}^d} \left(\dot{\overline{\psi}} + \dot{J}_{\mathcal{U}^d} \, J_{\mathcal{U}^d}^{-1} \, \overline{\psi} \right) \tag{26a}$$

where a routine calculation shows that

$$\dot{J}_{\mathcal{U}^d} \, J_{\mathcal{U}^d}^{-1} = \operatorname{tr}\left((\dot{\boldsymbol{\mathcal{U}}}^d)^T \, \boldsymbol{\mathcal{U}}^{d^{-1}} \right). \tag{26b}$$

Because the strain–energy function $\overline{\psi}$ is associated with an elastic deformation, its rate is given by the mechanical power induced by a rate of change in the elastic Laplace stretch at a material point. Therefore, the time-derivative of this strain–energy function $\overline{\psi}$ can be written as

$$\dot{\overline{\psi}} = \operatorname{tr}\left(\overline{\mathbf{P}}^T \, \dot{\boldsymbol{\mathcal{U}}}^e \right) = J_{\mathcal{U}^d} \operatorname{tr}\left(\left(\boldsymbol{\mathcal{P}} \, \boldsymbol{\mathcal{U}}^{d^T} \right)^T \dot{\boldsymbol{\mathcal{U}}}^e \right) \tag{27}$$

where $\overline{\mathbf{P}}$ being the first Piola–Kirchhoff stress pushed forward into the configuration $\bar{\kappa}_d(\mathcal{B})$ by $\overline{\mathbf{P}} = J_{\mathcal{U}^d}^{-1} \, \boldsymbol{\mathcal{P}} \, \boldsymbol{\mathcal{U}}^{d^T}$. Here $\boldsymbol{\mathcal{P}}$ is the first Piola–Kirchhoff stress in our physical frame of reference, and is obtained by pulling back the Cauchy stress defined in the current configuration $\bar{\kappa}_t(\mathcal{B})$. Now, a time-derivative of the relation $\boldsymbol{\mathcal{U}} = \boldsymbol{\mathcal{U}}^e \, \boldsymbol{\mathcal{U}}^d$ yields

$$\dot{\boldsymbol{\mathcal{U}}}^e = \dot{\boldsymbol{\mathcal{U}}} \, \boldsymbol{\mathcal{U}}^{d^{-1}} - \boldsymbol{\mathcal{U}}^e \, \dot{\boldsymbol{\mathcal{U}}}^d \, \boldsymbol{\mathcal{U}}^{d^{-1}}. \tag{28}$$

Substituting Eq. (28), the first part of Eq. (27) can be written as

$$\dot{\overline{\psi}} = J_{\mathcal{U}^d}^{-1} \left[\operatorname{tr}\left(\boldsymbol{\mathcal{P}}^T \, \dot{\boldsymbol{\mathcal{U}}} \right) - \operatorname{tr}\left((\boldsymbol{\mathcal{U}}^T \, \boldsymbol{\mathcal{P}})^T \, \dot{\boldsymbol{\mathcal{U}}}^d \, \boldsymbol{\mathcal{U}}^{d^{-1}} \right) \right]. \tag{29}$$

Substituting Eqs. (29) and (26b) into Eq. (26a), we arrive at

$$\dot{\hat{\psi}} = \operatorname{tr}\left(\boldsymbol{\mathcal{P}}^T \, \dot{\boldsymbol{\mathcal{U}}} \right) + \operatorname{tr}\left(\left(J_{\mathcal{U}^d} \, \overline{\psi} \, \boldsymbol{I} - \boldsymbol{\mathcal{U}}^T \, \boldsymbol{\mathcal{P}} \right)^T \dot{\boldsymbol{\mathcal{U}}}^d \, \boldsymbol{\mathcal{U}}^{d^{-1}} \right) \tag{30}$$

thereby allowing the Eshelby energy–momentum tensor to be redefined as

$$\boldsymbol{\mathcal{E}} := J_{\mathcal{U}^d} \, \overline{\psi} \, \boldsymbol{I} - \boldsymbol{\mathcal{U}}^T \, \boldsymbol{\mathcal{P}} = \hat{\psi} \, \boldsymbol{I} - \boldsymbol{\mathcal{U}}^T \, \boldsymbol{\mathcal{P}}. \tag{31}$$

In general, the Eshelby energy–momentum tensor $\boldsymbol{\mathcal{E}}$ need not be upper-triangular or symmetric; here we consider it to be a full matrix. One can clearly identify the similarity between Eq. (31) and Eshelby's energy–momentum identity (1) (cf. Epstein and Maugin (1996), Gupta et al. (2007)). Let us now understand the physical significance of the defined Eshelby energy–momentum tensor $\boldsymbol{\mathcal{E}}$ in the light of Eq. (30). To simplify, we rewrite Eq. (30) alternatively as

$$\operatorname{tr}\left(\boldsymbol{\mathcal{P}}^T \, \dot{\boldsymbol{\mathcal{U}}} \right) = \dot{\hat{\psi}} + \operatorname{tr}\left(\boldsymbol{\mathcal{E}}^T \, \dot{\boldsymbol{\mathcal{U}}}^d \, \boldsymbol{\mathcal{U}}^{d^{-1}} \right) = \dot{\hat{\psi}} + \operatorname{tr}\left(\boldsymbol{\mathcal{E}}^T \, \boldsymbol{\mathcal{L}}^d \right). \tag{32}$$

Using the relationship $\boldsymbol{\mathcal{P}} = \boldsymbol{\mathcal{S}} \, \boldsymbol{\mathcal{U}}^{-T}$, it can be easily observed that the left hand side of Eq. (32) represents the mechanical power at a

material point due to a loading of the body. Because the Helmholtz potential function ψ determines the energy stored in a body, the quantity $\mathrm{tr}(\boldsymbol{\mathcal{E}}^d\,\boldsymbol{\mathcal{L}}^d)$ must represent the energy that is being dissipated during an evolution of the natural configurations. The similarity of Eq. (17) and (32) also needs to be noticed in this connection. In view of the preceding discussion, we can now write

$$\mathrm{tr}\left(\boldsymbol{\mathcal{E}}^T\,\boldsymbol{\mathcal{L}}^d\right)=\xi. \tag{33}$$

From Eq. (33), it is evident that the rate of dissipation function, ξ can be interpreted as the stress power during the dissipative process and is associated with the change in microstructures of the body which results in an irreversible deformation. To use the full potential of an upper-triangular decomposition, we now deconstruct the rate of dissipation function into kinetic and kinematic attributes in a similar fashion as in Eq. (10). To do that, we first need to decompose the dissipative Laplace stretch in different modes of deformation. This decomposition is similar to the one derived by Freed (2017) and has already been used earlier to define the dissipative strain attributes in Eq. (16b). Nevertheless, we elaborate this decomposition here for the sake of completeness.

Because the dissipative part of Laplace stretch is an upper-triangular matrix, then using its group property it can be decomposed into a diagonal extension matrix followed by two matrices whose off-diagonal terms represent extents of shear. In particular, this decomposition can be written as

$$[\mathcal{U}^d_{ij}]=\underbrace{\begin{bmatrix}a^d&0&0\\0&b^d&0\\0&0&c^d\end{bmatrix}}_{\Lambda^d}\underbrace{\begin{bmatrix}1&0&\beta^d\\0&1&\alpha^d\\0&0&1\end{bmatrix}}_{\mathcal{U}^{d^{\alpha\beta}}}\underbrace{\begin{bmatrix}1&\gamma^d&0\\0&1&0\\0&0&1\end{bmatrix}}_{\mathcal{U}^{d^{\gamma}}}. \tag{34a}$$

Λ^d can be further decomposed as

$$\begin{aligned}[\Lambda^d_{ij}]=&\underbrace{\sqrt[3]{a^d\,b^d\,c^d}\,\lfloor 111\rfloor}_{\Lambda^d_0}\\&\times\underbrace{\left\lfloor\sqrt[3]{a^d/b^d}\quad\sqrt[3]{b^d/a^d}\quad 1\right\rfloor}_{\Lambda^d_{12}}\times\underbrace{\left\lfloor 1\quad\sqrt[3]{b^d/c^d}\quad\sqrt[3]{c^d/b^d}\right\rfloor}_{\Lambda^d_{23}}\\&\times\underbrace{\left\lfloor\sqrt[3]{a/c}\quad 1\quad\sqrt[3]{c^d/a^d}\right\rfloor}_{\Lambda^d_{31}}.\end{aligned} \tag{34b}$$

A routine calculation using Eq. (34b) shows that the velocity gradient associated with a dissipative process can be written as

$$\begin{aligned}\boldsymbol{\mathcal{L}}^d=\dot{\boldsymbol{\mathcal{U}}}^d\,\boldsymbol{\mathcal{U}}^{d^{-1}}=&\dot{\boldsymbol{\Lambda}}^d\,\boldsymbol{\Lambda}^{d^{-1}}+\boldsymbol{\Lambda}^d\,(\dot{\boldsymbol{\mathcal{U}}}^{d^{\alpha\beta}}\,\boldsymbol{\mathcal{U}}^{d^{\alpha\beta^{-1}}})\,\boldsymbol{\Lambda}^{d^{-1}}\\&+\boldsymbol{\mathcal{U}}^d\,(\dot{\boldsymbol{\mathcal{U}}}^{d^{\gamma}}\,\boldsymbol{\mathcal{U}}^{d^{\gamma^{-1}}})\,\boldsymbol{\mathcal{U}}^{d^{-1}}\end{aligned} \tag{35a}$$

with

$$\dot{\boldsymbol{\Lambda}}^d\,\boldsymbol{\Lambda}^{d^{-1}}=\dot{\boldsymbol{\Lambda}}^d_0\,\boldsymbol{\Lambda}^{d^{-1}}_0+\dot{\boldsymbol{\Lambda}}^d_{12}\,\boldsymbol{\Lambda}^{d^{-1}}_{12}+\dot{\boldsymbol{\Lambda}}^d_{23}\,\boldsymbol{\Lambda}^{d^{-1}}_{23}+\dot{\boldsymbol{\Lambda}}^d_{31}\,\boldsymbol{\Lambda}^{d^{-1}}_{31}. \tag{35b}$$

The fact that the products of diagonal matrices commute is instrumental in the derivation of Eq. (35b). The rate of dissipation function can now be written as

$$\begin{aligned}\xi&=\mathrm{tr}\left(\boldsymbol{\mathcal{E}}^T\,\boldsymbol{\mathcal{L}}^d\right)\\&=\mathrm{tr}(\boldsymbol{\mathcal{E}}^T\cdot\dot{\boldsymbol{\Lambda}}\,\boldsymbol{\Lambda}^{-1})+\mathrm{tr}(\boldsymbol{\Lambda}^{d^{-1}}\,\boldsymbol{\mathcal{E}}^T\,\boldsymbol{\Lambda}^d\cdot\dot{\boldsymbol{\mathcal{U}}}^{d^{\alpha\beta}}\,\boldsymbol{\mathcal{U}}^{d^{\alpha\beta^{-1}}})\\&\quad+\mathrm{tr}(\boldsymbol{\mathcal{U}}^{d^{-1}}\,\boldsymbol{\mathcal{E}}^T\,\boldsymbol{\mathcal{U}}^d\cdot\dot{\boldsymbol{\mathcal{U}}}^{d^{\gamma}}\,\boldsymbol{\mathcal{U}}^{d^{\gamma^{-1}}}).\end{aligned} \tag{36}$$

Now we consider the individual contributions for different modes of deformation to the rate of dissipation function ξ. Because $\boldsymbol{\Lambda}$ is a diagonal matrix, its contribution to the rate of dissipation is given by

$$\xi^{\Lambda}=\mathrm{tr}(\boldsymbol{\mathcal{E}}^T\cdot\dot{\boldsymbol{\Lambda}}\,\boldsymbol{\Lambda}^{-1})=\mathcal{E}_{11}\,\frac{\dot{a}^d}{a^d}+\mathcal{E}_{22}\,\frac{\dot{b}^d}{b^d}+\mathcal{E}_{33}\,\frac{\dot{c}^d}{c^d}. \tag{37}$$

This contribution can be further decomposed into dilatation and squeeze modes in accordance with Eq. (35b) as[2]

Dilatation:

$$\xi^{\Lambda_0}=\mathrm{tr}(\boldsymbol{\mathcal{E}}^T\cdot\dot{\boldsymbol{\Lambda}}_0\,\boldsymbol{\Lambda}_0^{-1})=(\mathcal{E}_{11}+\mathcal{E}_{22}+\mathcal{E}_{33})\times\frac{1}{3}\left(\frac{\dot{a}^d}{a^d}+\frac{\dot{b}^d}{b^d}+\frac{\dot{c}^d}{c^d}\right); \tag{38a}$$

1-2 squeeze:

$$\xi^{\Lambda_{12}}=\mathrm{tr}(\boldsymbol{\mathcal{E}}^T\cdot\dot{\boldsymbol{\Lambda}}_{12}\,\boldsymbol{\Lambda}_{12}^{-1})=(\mathcal{E}_{11}-\mathcal{E}_{22})\times\frac{1}{3}\left(\frac{\dot{a}^d}{a^d}-\frac{\dot{b}^d}{b^d}\right); \tag{38b}$$

2-3 squeeze:

$$\xi^{\Lambda_{23}}=\mathrm{tr}(\boldsymbol{\mathcal{E}}^T\cdot\dot{\boldsymbol{\Lambda}}_{23}\,\boldsymbol{\Lambda}_{23}^{-1})=(\mathcal{E}_{22}-\mathcal{E}_{33})\times\frac{1}{3}\left(\frac{\dot{b}^d}{b^d}-\frac{\dot{c}^d}{c^d}\right); \tag{38c}$$

3-1 squeeze:

$$\xi^{\Lambda_{31}}=\mathrm{tr}(\boldsymbol{\mathcal{E}}^T\cdot\dot{\boldsymbol{\Lambda}}_{31}\,\boldsymbol{\Lambda}_{31}^{-1})=(\mathcal{E}_{33}-\mathcal{E}_{11})\times\frac{1}{3}\left(\frac{\dot{c}^d}{a^d}-\frac{\dot{a}^d}{c^d}\right). \tag{38d}$$

Similarly for the shear modes, the contribution to the rate of dissipation can be written as

$$\xi^{\mathcal{U}^{\alpha\beta}}=\mathrm{tr}(\boldsymbol{\Lambda}^{d^{-1}}\,\boldsymbol{\mathcal{E}}^T\,\boldsymbol{\Lambda}^d\cdot\dot{\boldsymbol{\mathcal{U}}}^{d^{\alpha\beta}}\,\boldsymbol{\mathcal{U}}^{d^{\alpha\beta^{-1}}})=\frac{b^d}{c^d}\,\mathcal{E}_{23}\times\dot{\alpha}^d+\frac{a^d}{c^d}\,\mathcal{E}_{13}\times\dot{\beta}^d \tag{38e}$$

and

$$\xi^{\mathcal{U}^{\gamma}}=\mathrm{tr}(\boldsymbol{\mathcal{U}}^{d^{-1}}\,\boldsymbol{\mathcal{E}}^T\,\boldsymbol{\mathcal{U}}^d\cdot\dot{\boldsymbol{\mathcal{U}}}^{d^{\gamma}}\,\boldsymbol{\mathcal{U}}^{d^{\gamma^{-1}}})=\left(\frac{a^d}{b^d}\mathcal{E}_{12}-\alpha^d\,\frac{a^d}{c^d}\mathcal{E}_{13}\right)\times\dot{\gamma}^d. \tag{38f}$$

It is now possible to write the rate of dissipation function ξ as a sum of contributions from different modes of deformation as

$$\xi=-\rho_0\,\frac{\partial\psi}{\partial\delta^d}\,\dot{\delta}^d-\rho_0\sum_{i=1}^{3}\left(\frac{\partial\psi}{\partial\epsilon^d_i}\,\dot{\epsilon}^d_i+\frac{\partial\psi}{\partial\gamma^d_i}\,\dot{\gamma}^d_i\right)=\pi^d\,\dot{\delta}^d+\sum_{i=1}^{3}\left(\sigma^d_i\,\dot{\epsilon}^d_i+\tau^d_i\,\dot{\gamma}^d_i\right) \tag{39}$$

where the dissipative strain attributes are defined according to Eq. (13b), while the driving force attributes can be written in terms of the components of the Eshelby's energy–momentum tensor as

$$\begin{aligned}&\pi^d=\mathcal{E}_{11}+\mathcal{E}_{22}+\mathcal{E}_{33};\quad\sigma^d_1=\mathcal{E}_{11}-\mathcal{E}_{22};\quad\sigma^d_2=\mathcal{E}_{22}-\mathcal{E}_{33};\\&\sigma^d_3=\mathcal{E}_{33}-\mathcal{E}_{11};\\&\tau^d_1=\frac{b^d}{c^d}\,\mathcal{E}_{23};\quad\tau^d_2=\frac{a^d}{c^d}\,\mathcal{E}_{13};\quad\tau^d_3=\left(\frac{a^d}{b^d}\mathcal{E}_{12}-\alpha^d\,\frac{a^d}{c^d}\mathcal{E}_{13}\right).\end{aligned} \tag{40}$$

It is worth noting that the rate of dissipation function ξ was previously expressed in terms of the tensorial kinematic and kinetic variables, viz., the dissipative velocity gradient $\boldsymbol{\mathcal{L}}^d$ and the Eshelby energy–momentum tensor $\boldsymbol{\mathcal{E}}$ respectively in Eq. (33). However, the use of an upper-triangular decomposition in the deconstruction of ξ enables us to express it in terms of the corresponding scalar conjugate variables. Needless to say that the use of scalar conjugate variables greatly facilitates the construction of constitutive model in terms of the ease of computation. The driving force attributes, thus defined, must also follow their definitions (Eq. (24b)), which are obtained from thermodynamic consideration. Moreover, even though a form for the Helmholtz potential function is assumed, we still need to determine the evolution equations for the dissipative strain rate attributes. The constitutive formulations for the dissipative strain rates will be developed in the next section.

Now we will show that the definitions of the driving force attributes in Eq. (24b) is also consistent with the ones derived from a deconstruction of the rate of dissipation ξ. Let us consider that the elastic response of the material is that of a Green elastic solid. Therefore, the

[2] A routine calculation shows that the kinematic counterparts of the corresponding driving force attributes are consistent with the ones defined in Eq. (15).

stress attributes can be obtained from the derivatives of the Helmholtz potential ψ with respect to the corresponding strain attributes, i.e.,

$$\pi = \rho_0 \frac{\partial \psi}{\partial \delta}; \quad \sigma_i = \rho_0 \frac{\partial \psi}{\partial \epsilon_i}; \quad \tau_i = \rho_0 \frac{\partial \psi}{\partial \gamma_i}, \text{ where } i = 1, 2, 3. \tag{41}$$

Substituting Eqs. (18) and (19) into (17) and using (41), one can easily recover Eq. (39).

3.3. Anisotropic materials

In our derivation, we have assumed so far that the material remains isotropic throughout the deformation process. Therefore, the dissipative strain rate attributes are related to the components of the velocity gradient associated with the dissipative process through Eq. (15). In this case, the driving force attributes can be written in terms of the components of the Eshelby energy–momentum tensor as

$$\begin{Bmatrix} \pi^d \\ \sigma_1^d \\ \sigma_2^d \\ \tau_1^d \\ \tau_2^d \\ \tau_3^d \end{Bmatrix} = \begin{bmatrix} 1 & 1 & 1 & 0 & 0 & 0 \\ 1 & -1 & 0 & 0 & 0 & 0 \\ 0 & 1 & -1 & 0 & 0 & 0 \\ 0 & 0 & 0 & b^d/c^d & 0 & 0 \\ 0 & 0 & 0 & 0 & a^d/c^d & 0 \\ 0 & 0 & 0 & 0 & -\alpha^d a^d/c^d & a^d/b^d \end{bmatrix} \begin{Bmatrix} \mathcal{E}_{11} \\ \mathcal{E}_{22} \\ \mathcal{E}_{33} \\ \mathcal{E}_{23} \\ \mathcal{E}_{13} \\ \mathcal{E}_{12} \end{Bmatrix}. \tag{42}$$

Unlike the relationship between the stress attributes l_σ and the components of the Piola–Kirchhoff stress $\boldsymbol{S}$, the inversion of relation (45) does not provide all the components of the Eshelby tensor, $\boldsymbol{\mathcal{E}}$. This is due to the fact that *the components of the Eshelby tensor $\boldsymbol{\mathcal{E}}$ below the diagonal do not contribute to the energy dissipated from the system, whereas the driving force attributes are obtained from a deconstruction of the rate of dissipation function*. This is a direct consequence of using an upper-triangular decomposition (see Appendix). This condition is similar to a well-known fact in the classical theory that the thermodynamic contribution of a spin tensor in conjunction with a symmetric stress tensor is zero. In general, one can only find the lower-triangular components of the tensorial kinetic quantity such as the Kirchhoff stress, $\boldsymbol{S}$ or the Eshelby tensor $\boldsymbol{\mathcal{E}}$ from the kinetic attributes, e.g., the stress attributes l_σ or the driving force attributes l_{σ^d}. Only in the case of a symmetric or lower-triangular tensor-valued kinetic quantity, it is possible to find all the components of the kinematic quantity from its respective attributes.

Many materials exhibit an evolving anisotropy throughout the dissipative process, e.g., plastically-induced anisotropy in metal plasticity (Van der Giessen, 1989, 1991). In our framework, this anisotropy enters into our constitutive formulation through the map between the kinematic or kinetic attributes and their tensorial counterparts. In particular, the dissipative strain rate attributes are related to the components of $\boldsymbol{\mathcal{L}}^d$ via

$$\begin{Bmatrix} \dot{\delta}^d \\ \dot{\epsilon}_1^d \\ \dot{\epsilon}_2^d \\ \dot{\gamma}_1^d \\ \dot{\gamma}_2^d \\ \dot{\gamma}_3^d \end{Bmatrix} = \begin{bmatrix} vw/3u & uw/3v & uv/3w & 0 & 0 & 0 \\ vw/3u & -uw/3v & 0 & 0 & 0 & 0 \\ 0 & uw/3v & -uv/3w & 0 & 0 & 0 \\ 0 & 0 & 0 & c^d/b^d & 0 & 0 \\ 0 & 0 & 0 & 0 & c^d/a^d & b^d\alpha^d/a^d \\ 0 & 0 & 0 & 0 & 0 & b^d/a^d \end{bmatrix} \times \begin{Bmatrix} \mathcal{L}_{11}^d \\ \mathcal{L}_{22}^d \\ \mathcal{L}_{33}^d \\ \mathcal{L}_{23}^d \\ \mathcal{L}_{13}^d \\ \mathcal{L}_{12}^d \end{Bmatrix}. \tag{43}$$

Here u, v and w are the anisotropy parameters that denote the strength of the material along a coordinate direction in our physical frame of reference over that in the other two directions.[3] To incorporate an involving anisotropy, one must consider u, v and w as kinematic variables. Following the derivation in Section 3.2, the relation between the driving force attributes and the components of the Eshelby energy–momentum tensor, on or above the matrix diagonal,[4] can be written as

$$\begin{Bmatrix} \pi^d \\ \sigma_1^d \\ \sigma_2^d \\ \tau_1^d \\ \tau_2^d \\ \tau_3^d \end{Bmatrix} = \begin{bmatrix} u/vw & v/uw & w/uv & 0 & 0 & 0 \\ u/vw & -v/uw & 0 & 0 & 0 & 0 \\ 0 & v/uw & -w/uv & 0 & 0 & 0 \\ 0 & 0 & 0 & b^d/c^d & 0 & 0 \\ 0 & 0 & 0 & 0 & a^d/c^d & 0 \\ 0 & 0 & 0 & 0 & -\alpha^d a^d/c^d & a^d/b^d \end{bmatrix} \times \begin{Bmatrix} \mathcal{E}_{11} \\ \mathcal{E}_{22} \\ \mathcal{E}_{33} \\ \mathcal{E}_{23} \\ \mathcal{E}_{13} \\ \mathcal{E}_{12} \end{Bmatrix}. \tag{44}$$

Conversely, the components of the Eshelby energy–momentum tensor can be expressed in terms of the driving force attributes as

$$\begin{Bmatrix} \mathcal{E}_{11} \\ \mathcal{E}_{22} \\ \mathcal{E}_{33} \\ \mathcal{E}_{23} \\ \mathcal{E}_{13} \\ \mathcal{E}_{12} \end{Bmatrix} = \begin{bmatrix} vw/3u & 2vw/3u & vw/3u & 0 & 0 & 0 \\ uw/3v & -uw/3v & uw/3v & 0 & 0 & 0 \\ uv/3w & -uv/3w & -2uv/3w & 0 & 0 & 0 \\ 0 & 0 & 0 & c^d/b^d & 0 & 0 \\ 0 & 0 & 0 & 0 & c^d/a^d & 0 \\ 0 & 0 & 0 & 0 & b^d\alpha^d/a^d & b^d/a^d \end{bmatrix} \times \begin{Bmatrix} \pi^d \\ \sigma_1^d \\ \sigma_2^d \\ \tau_1^d \\ \tau_2^d \\ \tau_3^d \end{Bmatrix}. \tag{45}$$

4. Constitutive relations

With the driving force attributes defined in the preceding section, we now need to determine the evolution equations for the dissipative strain rate attributes. It is well-known that the second law of thermodynamics provides a weak guidance on deriving the evolution equations for kinematic (or kinetic) variables whenever a dissipative process is involved. To resolve this issue, a number of more stringent criteria have to be employed. Different balance laws for the configurational forces constitute a large portion of these criteria. Other criteria have also been used in specific fields of application. For example, the use of maximum plastic work criterion, Drucker's stability postulate, and a maximum plastic dissipation criterion are abundant in the plasticity

[3] Although the parameters u, v and w are initially introduced in the encoding/decoding map of the kinetic variables (hence, the material response), one must ensure that the stress power remains unaltered. Therefore, these parameters also enter into the encoding/decoding map of the kinematics variables. The reader is referred to Erel and Freed (2017) and Freed (2017) for further details.

[4] Note that, in general, only the elements located on or below the matrix diagonal contribute to the trace of its product with an upper-triangular matrix. In this case, however, the transpose of $\boldsymbol{\mathcal{E}}$ has been used to determine the rate of dissipation function ξ. Therefore, an inversion of the above relation provides the upper-triangular elements of $\boldsymbol{\mathcal{E}}$.

literature (Lubliner, 2008; Simo and Hughes, 2006). Here we adopt the maximum rate of dissipation principle proposed by Rajagopal and Srinivasa (1998, 2004) because of its wider range of application and suitability to the framework of multiple natural configurations. This criterion is in sync with Onsager's minimum rate of entropy production (Onsager, 1931) and Ziegler's normality rule (Ziegler, 1963). According to this criterion, among the admissible kinematic (or kinetic) quantities, the path that maximizes the rate of dissipation ξ is selected to govern evolution of the natural configurations. The admissible kinematic (or kinetic) quantities are the ones that satisfy the energy balance Eq. (17) or, its reduced form (39). For the time being, we assume that the rate of dissipation ξ is a convex and sufficiently smooth function such that its derivatives can be obtained at any values of its arguments.

In the development of constitutive formulation, we first allow the kinematic variables, i.e., the dissipative strain rate attributes, to vary while keeping the driving force attributes fixed. Because ξ is sufficiently smooth, maximization of the rate of dissipation ξ can be carried out by using a Langrange multiplier technique. Here Eq. (39) acts as a constraint. The maximization of ξ with respect to the dissipative strain rate attributes $l_{\dot{\mathcal{U}}^d}$ yields[5]

$$\pi^d = \lambda \frac{\partial \hat{\xi}}{\partial \dot{\delta}^d}; \quad \sigma_i^d = \lambda \frac{\partial \hat{\xi}}{\partial \dot{\epsilon}_i^d}; \quad \tau_i^d = \lambda \frac{\partial \hat{\xi}}{\partial \dot{\gamma}_i^d}, \quad i = 1,2,3 \tag{46}$$

where λ is the Lagrange multiplier that can be found by the satisfaction of Eq. (39). Note that Eq. (46) is a set of implicit equations in $l_{\dot{\mathcal{U}}^d}$. The derivation of constitutive relations, so far, closely follows Paul and Freed (2021), and details of this derivation can be found there. Although their model was developed for a specific application, the model constructed here is valid for any dissipative system whose deformation can be explained via a multiplicative decomposition of a kinematic quantity such as a deformation gradient, or a Laplace stretch.

A significant departure from Paul and Freed's (2021) constitutive formulation is realized when the correct causality is considered. Because the kinetic (stress or driving force) and kinematic (strain) attributes act as "determinant" and "resultant", respectively, the kinematic attributes should be held fixed while the kinetic attributes are allowed to vary (Rajagopal and Srinivasa, 2019). In the work of Paul and Freed (2021), it was necessary to assume a special form for the Helmholtz potential function[6] to derive explicit expressions for the dissipative strain rate attributes $l_{\dot{\mathcal{U}}^d}$. This is due to the fact that derivatives of the Helmholtz potential function taken with respect to the dissipative (plastic) strain attributes lack physical interpretation without consideration of Eshelby's energy–momentum tensor. In view of the driving force attributes, no such assumption is required in our constitutive formulation. The explicit evolution equations for $l_{\dot{\mathcal{U}}^d}$ can be obtained directly through a maximization of the rate of dissipation function ξ taken with respect to the driving force attributes l_{σ^d}. Eq. (39) acts as a constraint in this optimization process. Carrying out this optimization process, using a Lagrange multiplier technique, one readily obtains

$$\dot{\delta}^d = \mu \frac{\partial \hat{\xi}}{\partial \pi^d}; \quad \dot{\epsilon}_i^d = \mu \frac{\partial \hat{\xi}}{\partial \sigma_i^d}; \quad \dot{\gamma}_i^d = \mu \frac{\partial \hat{\xi}}{\partial \tau_i^d}. \tag{47}$$

The Lagrange multiplier μ can be found from a satisfaction of the reduced rate of dissipation equation (39).

Let us now understand the geometric significance of Eq. (47). It is evident that l_{σ^d} forms a six-dimensional space corresponding to different modes of deformation. Although there are seven driving stress attributes listed in l_{σ^d}, recall that a coupling exists between the three squeeze modes such that any one of the three driving force attributes σ_i^d can be expressed as a linear combination of the other two. This results in a reduction in the number of dimensions of the driving force attributes-space. Because the dissipative strain rate attributes are held fixed, the rate of dissipation function ξ can be viewed as a surface in this six-dimensional space.

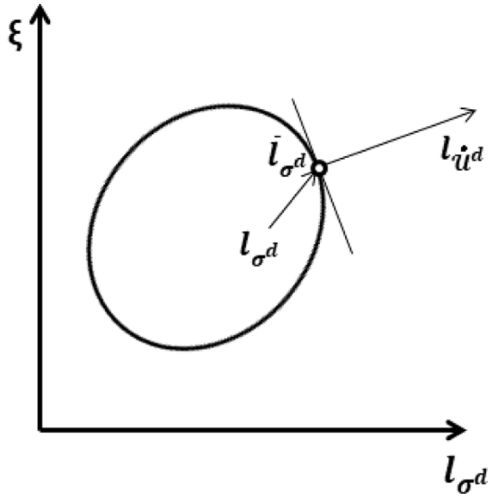

Fig. 2. Geometric interpretation of the normality condition. In a six-dimensional space l_{σ^d}, the dissipative strain rate attributes must be along the normal to the rate of dissipation function at $\bar{l}_{\sigma^d}$.

Because the rate of dissipation is a convex function in the driving force attributes-space, the normal to the rate of dissipation surface at a point is given by its derivative with respect to a driving force attribute at that point. Therefore, it is evident from Eq. (47) that *for each mode of deformation, the dissipative strain rate attributes are along the normal to the rate of dissipation function in a six-dimensional driving force attributes space* l_{σ^d} (see Fig. 2). This geometric meaning will be particularly useful in deriving the constitutive relations for materials in which the rate of dissipation is a continuous function, but not sufficiently smooth.

If the rate of dissipation function is non-differentiable at $l_{\sigma^d} = \mathbf{0}$, then we cannot use the Lagrange multiplier technique to derive the evolution equations for the dissipative strain rate attributes. Instead, it is possible to obtain a like result by using standard methods of convex analysis. The only assumption in this method is that the rate of dissipation function must be continuous and convex in the driving force attributes-space. Let us consider a fixed set of values for the dissipative strain rate attributes $l_{\dot{\mathcal{U}}^d}$ and two sets of values for the driving force attributes $\bar{l}_{\sigma^d}$ and l_{σ^d}. The values of $\bar{l}_{\sigma^d}$ and l_{σ^d} are chosen in such a way that they generate rates of dissipation in conjunction with the prescribed dissipative strain attributes $l_{\dot{\mathcal{U}}^d}$ satisfying $\xi(\bar{l}_{\sigma^d}, l_{\dot{\mathcal{U}}^d}) \geq \xi(l_{\sigma^d}, l_{\dot{\mathcal{U}}^d})$. Therefore, using Eq. (39), one can write this inequality as

$$(\pi^d - \bar{\pi}^d)\,\delta^d + \sum_{i=1}^{3} \left[(\sigma_i^d - \bar{\sigma}_i^d)\,\epsilon_i^d + (\tau_i^d - \bar{\tau}_i^d)\,\gamma_i^d \right] \leq 0. \tag{48}$$

Let us define the convex hull in the driving force attributes space as

$$\mathbb{C}_{l_{\sigma^d}} = c_0\,\pi^d + \sum_{i=1}^{3} (c_i\,\sigma_i^d + c_{i+3}\,\tau_i^d) \quad \text{with } c_0, c_1, \ldots, c_6 \geq 0, \sum_{i=0}^{6} c_i = 1. \tag{49}$$

Geometrically, the convex hull $\mathbb{C}_{l_{\sigma^d}}$ constitutes all straight lines whose ends form the set l_{σ^d}, i.e., a set of all admissible driving force attributes. From Eq. (48), it is evident that the dissipative strain attributes do not make an acute angle with the driving force attributes $\bar{l}_{\sigma^d}$ with l_{σ^d} as endpoints (see Fig. 2). Therefore, *the dissipative strain rate attributes* $l_{\dot{\mathcal{U}}^d}$ *are along the normal cone to the convex hull* $\mathbb{C}_{l_{\sigma^d}}$ *at* $\bar{l}_{\sigma^d}$. This statement is similar to the physical meanings of the evolution equations of $l_{\dot{\mathcal{U}}^d}$ in case of a smooth rate of dissipation function. Nevertheless, the

[5] See Paul and Freed (2021) for a detailed derivation.

[6] Instead of the Helmholtz potential function, one should use a Gibbs potential when the kinetic attributes are allowed to vary, because the Helmholtz potential function essentially depends on the kinematic variables. A Gibbs potential can be easily obtained from the Helmholtz potential function through its Legendre transformation.

evolution equations in the latter are more tractable, as it is possible to derive explicit evolution equations for the dissipative strain attributes *separately* for each mode of deformation. On the other hand, a convex analysis provides an evolution equation for the dissipative strain attributes in a consolidated form.

4.1. Example: Classical J_2 plasticity

In this section, we illustrate the developed theory with an example of classical J_2 plasticity. Under the application of load, an elastic–plastic material undergoes an irreversible deformation due to changes in microstructure such as dislocation motion. The deformed body is further subjected to an elastic stretch and an elastic rotation. Clearly, the change in microstructure and the resulting irreversible deformation is a dissipative process. Hence, the mechanical response of an elastic–plastic material can be modeled within the framework of multiple natural configurations. Here a plastic deformation takes the reference configuration of the body into its natural configuration. Therefore, the evolution of this natural configuration is governed by the strain rate attributes associated with a dissipative, plastic deformation. Although J_2 plasticity is typically developed within the small-strain framework, we can develop a similar but finite theory here, because in our theory the total strain can be additively decomposed into elastic and plastic parts as per Eq. (14).

Following the developments in Section 2 and Section 3, we can now define the plastic strain rate attributes, stress attributes, and the driving force attributes in a similar fashion as in Eqs. (13b), (9a)–(9g) and, (24b). Here we replace the superscript '$\square^d$' by '$\square^p$' to denote the plastic deformation. In J_2 plasticity, it is assumed that a material undergoes a plastic deformation whenever a quantity J_2 associated with the deviatoric part of the Cauchy stress reaches the yield stress in shear, k. J_2 is often referred to as the Mises stress. Tacit in this assumption is that the plastic deformation does not depend on the dilatational mode of deformation. We further assume that the material remains isotropic throughout the deformation process. To develop the J_2 plasticity theory in our framework, we need to specify a constitutive assumption for the rate of dissipation function ξ. ξ can be assumed to be a function of either the driving force attributes or the plastic strain rate attributes depending on the nature of variables (kinematic or, kinetic) being held at a fixed value.

If the kinetic variables are held fixed while the kinematic variables are allowed to vary, then the rate of dissipation function is assumed to be a function of the plastic squeeze strain rate attributes, $\dot{\varepsilon}_i^p$, and plastic shear strain rate attributes, $\dot{\gamma}_i^p$. Specifically, we assume that the rate of dissipation has the form

$$\xi = k\sqrt{\sum_{i=1}^{3}\left(\dot{\varepsilon}_i^{p^2} + \dot{\gamma}_i^{p^2}\right)}. \tag{50}$$

Notice that the rate of dissipation function is not dependent upon the dilatational plastic strain attribute, $\dot{\delta}_i^p$. This ensures that the plastic deformation process is volume-conserving. Now using Eq. (46), one can easily find the driving force attributes as

$$\sigma_i^p = \frac{k\dot{\varepsilon}_i^p}{\sqrt{\sum_{i=1}^{3}\left(\dot{\varepsilon}_i^{p^2} + \dot{\gamma}_i^{p^2}\right)}}; \quad \tau_i^p = \frac{k\dot{\gamma}_i^p}{\sqrt{\sum_{i=1}^{3}\left(\dot{\varepsilon}_i^{p^2} + \dot{\gamma}_i^{p^2}\right)}}, \quad i = 1,2,3. \tag{51}$$

Because the driving force attributes σ_i^p and τ_i^p are responsible for the dissipative, plastic deformation process, and act as the thermodynamic conjugates to the plastic strain rate attributes, we can now define a quantity $\mathcal{J}_2$ as

$$\mathcal{J}_2 := \sqrt{\sum_{i=1}^{3}\left(\sigma_i^{p^2} + \tau_i^{p^2}\right)}. \tag{52}$$

Needless to say that the quantity $\mathcal{J}_2$ is equivalent to the Mises stress in classical plasticity theory. It is important to note that for a set of plastic strain rate attributes and driving force attributes to be admissible, they must satisfy the reduced rate of dissipation constraint (39). Thus, the yield condition can now be defined as

$$\begin{aligned} &\frac{\sigma_i^p\,\dot{\delta}_i^p + \sum_{i=1}^{3}\left(\sigma_i^p\,\dot{\varepsilon}_i^p + \tau_i^p\,\dot{\gamma}_i^p\right)}{\xi} < 1; \quad \text{when the deformation is elastic;} \\ &\frac{\sigma_i^p\,\dot{\delta}_i^p + \sum_{i=1}^{3}\left(\sigma_i^p\,\dot{\varepsilon}_i^p + \tau_i^p\,\dot{\gamma}_i^p\right)}{\xi} = 1; \quad \text{the material yields.} \end{aligned} \tag{53}$$

Substituting driving force attributes from Eq. (52) into Eq. (53) and using the definition of $\mathcal{J}_2$, one can easily find that

$$\mathcal{J}_2 = k \implies \mathcal{J}_2/k = 1. \tag{54}$$

It is important to note that whenever the Helmholtz potential is assumed to be a quadratic function of the difference between the total strain attributes and their corresponding plastic parts, then the driving force attributes for each mode of deformation is same as the corresponding stress attributes. This is due to the fact that Eshelby's energy–momentum tensor can be viewed as a dual of the Cauchy stress tensor (Maugin, 2016). With this assumption in place, one can easily check that the constitutive relations reduce to the ones derived by Paul and Freed (2021, § 5.1).

Now let us consider the other case where the plastic strain rate attributes are held fixed while the driving force attributes are allowed to vary. In this case, we assume that the elastic response of the body is that of a Green elastic solid. Note that this assumption gives us only a functional form for the Helmholtz potential function. The rate of dissipation ξ must be a function of the driving force attributes. Specifically, the rate of dissipation is written as

$$\xi = m\sqrt{\sum_{i=1}^{3}\left(\sigma_i^{p^2} + \tau_i^{p^2}\right)} \tag{55}$$

where m is a constant. From Eq. (47), the plastic strain rate attributes can be written as

$$\dot{\varepsilon}_i^p = \frac{m\sigma_i^p}{\sqrt{\sum_{i=1}^{3}\left(\sigma_i^{p^2} + \tau_i^{p^2}\right)}}; \quad \dot{\gamma}_i^p = \frac{m\tau_i^p}{\sqrt{\sum_{i=1}^{3}\left(\sigma_i^{p^2} + \tau_i^{p^2}\right)}}, \quad i = 1,2,3. \tag{56}$$

Using Eq. (53), it can be easily shown that the yield condition in this case is the same as Eq. (54).

5. Summary

In this paper, we examine the role of Eshelby's energy–momentum tensor in the context of **QR** kinematics. The primary advantage of using **QR** kinematics in constitutive formulation is that it is possible to construct constitutive models using scalar, conjugate, stress/strain, base pairs. These conjugate base pairs also have minimal coupling between them that helps when parametrizing a material model from an experimental standpoint. Although the concept of Eshelby's energy–momentum tensor has a wide range of mechanics applications, here we confine our attention to deformation processes that can be expressed through a multiplicative decomposition of the deformation gradient. Following Eshelby's method, we have derived driving force attributes that act as thermodynamic conjugates to the dissipative strain rate attributes. A one-to-one relationship has been established between these driving force attributes and the components of Eshelby's energy–momentum tensor. Finally, we study the role of these driving force attributes in construction of constitutive models.

Declaration of competing interest

The authors declare that they have no known competing financial interests or personal relationships that could have appeared to influence the work reported in this paper.

Appendix. Property of triangular matrices

In this section, we show that *if* **A** *and* **B** *are a full and an upper-triangular matrix respectively, then the trace of the matrix* **AB** *consists of only the lower-triangular components of the matrix* **A**. A full matrix **A** can always be decomposed uniquely into a lower-triangular matrix $\mathbf{A}_l$ and an upper-triangular matrix $\mathbf{A}_u$ whose diagonal elements are zero, i.e.,

$$\mathbf{A} = \begin{bmatrix} A_{11} & A_{12} & A_{13} \\ A_{21} & A_{22} & A_{23} \\ A_{31} & A_{32} & A_{33} \end{bmatrix} = \underbrace{\begin{bmatrix} A_{11} & 0 & 0 \\ A_{21} & A_{22} & 0 \\ A_{31} & A_{32} & A_{33} \end{bmatrix}}_{\mathbf{A}_l} + \underbrace{\begin{bmatrix} 0 & A_{12} & A_{13} \\ 0 & 0 & A_{23} \\ 0 & 0 & 0 \end{bmatrix}}_{\mathbf{A}_u}. \tag{A.1}$$

Proof of uniqueness: Let us consider that for a full matrix **A**, two such decompositions are possible such that

$$\mathbf{A} = \mathbf{A}_l + \mathbf{A}_u = \bar{\mathbf{A}}_l + \bar{\mathbf{A}}_u. \tag{A.2}$$

From Eq. (A.2), one can write

$$\mathbf{A}_l - \bar{\mathbf{A}}_l = \bar{\mathbf{A}}_u - \mathbf{A}_u. \tag{A.3}$$

Because the set of all triangular matrices are closed under addition, the left hand side of Eq. (A.3) is a lower-triangular matrix whereas its right hand side is an upper-triangular matrix with zero diagonal elements. A term-by-term comparison of the matrices in the left and right hand side of Eq. (A.3) implies that each element of these matrices must be zero. Therefore, each element in $\mathbf{A}_l$ and $\bar{\mathbf{A}}_l$, and $\mathbf{A}_u$ and $\bar{\mathbf{A}}_u$ should be equal. Because $\bar{\mathbf{A}}_l$ and $\bar{\mathbf{A}}_u$ are otherwise arbitrary triangular matrices, the decomposition in Eq. (A.1) must be unique.

Now, we use the properties of trace of a matrix to write

$$\mathrm{tr}(\mathbf{AB}) = \mathrm{tr}(\mathbf{A}_l\mathbf{B}) + \mathrm{tr}(\mathbf{A}_u\mathbf{B}). \tag{A.4}$$

Now product of the matrices $\mathbf{A}_u$ and **B** can be written as

$$\begin{aligned} \mathbf{A}_u\mathbf{B} &= \begin{bmatrix} 0 & A_{12} & A_{13} \\ 0 & 0 & A_{23} \\ 0 & 0 & 0 \end{bmatrix} \begin{bmatrix} B_{11} & B_{12} & B_{13} \\ 0 & B_{22} & B_{23} \\ 0 & 0 & B_{33} \end{bmatrix} \\ &= \begin{bmatrix} 0 & A_{12}B_{22} & A_{12}B_{23} + A_{13}B_{33} \\ 0 & 0 & A_{23}B_{33} \\ 0 & 0 & 0 \end{bmatrix}. \end{aligned} \tag{A.5}$$

Clearly, the trace of $\mathbf{A}_u\mathbf{B}$ is always zero for any values of the elements in $\mathbf{A}_u$ and **B**. Therefore, the only contribution to the trace of the matrix **AB** will come from the lower-triangular part of the matrix **A**. In the same way, one can show that the same property holds for $\mathrm{tr}(\boldsymbol{A}^T\boldsymbol{B})$. It is obvious that $\mathrm{tr}(\boldsymbol{A}^T\boldsymbol{B})$ consists of only the lower-triangular components of the matrix $\boldsymbol{A}^T$, i.e., in other words, the upper-triangular components of the matrix $\boldsymbol{A}$.

References

Avazmohammadi, Reza, Li, David S, Leahy, Thomas, Shih, Elizabeth, Soares, João S, Gorman, Joseph H, Gorman, Robert C, Sacks, Michael S, 2018. An integrated inverse model-experimental approach to determine soft tissue three-dimensional constitutive parameters: application to post-infarcted myocardium. Biomech. Model. Mechanobiol. 17 (1), 31–53.

Broerse, Taco, Krstekanić, Nemanja, Kasbergen, Cor, Willingshofer, Ernst, 2021. Mapping and classifying large deformation from digital imagery: application to analogue models of lithosphere deformation. Geophys. J. Int. 226 (2), 984–1017.

Cermelli, Paolo, Fried, Eliot, Sellers, Shaun, 2001. Configurational stress, yield and flow in rate–independent plasticity. Proc. R. Soc. Lond. Ser. A Math. Phys. Eng. Sci. 457 (2010), 1447–1467.

Clayton, J.D., Freed, A.D., 2020a. A constitutive framework for finite viscoelasticity and damage based on the Gram–Schmidt decomposition. Acta Mech. 231 (8), 3319–3362.

Clayton, John D., Freed, A.D., 2020b. A constitutive model for lung mechanics and injury applicable to static, dynamic, and shock loading. Mech. Soft Mater. 2 (1), 1–35.

Cleja-Tigoiu, S., Maugin, G.A., 2000. Eshelby's stress tensors in finite elastoplasticity. Acta Mech. 139 (1), 231–249.

Criscione, John C., 2004. Rivlin's representation formula is ill-conceived for the determination of response functions via biaxial testing. In: The Rational Spirit in Modern Continuum Mechanics. Springer, pp. 197–215.

Epstein, M., Maugin, G.A., 1990. The energy-momentum tensor and material uniformity in finite elasticity. Acta Mech. 83 (3–4), 127–133.

Epstein, M., Maugin, G.A., 1996. On the geometrical material structure of anelasticity. Acta Mech. 115 (1–4), 119–131.

Erel, V., Freed, A.D., 2017. Stress/strain basis pairs for anisotropic materials. Composites B 120, 152–158.

Erel, Veysel, Jiang, Mingliang, Moreno, Michael R., Freed, Alan D., 2019. Anisotropic conjugate stress/strain base pair approach for laminates undergoing large deformations. Materialia 6, 100318.

Eshelby, John Douglas, 1951. The force on an elastic singularity. Phil. Trans. R. Soc. A 244 (877), 87–112.

Eshelby, J.D., 1956. The continuum theory of lattice defects. Solid State Phys. 3, 79–144.

Eshelby, J.D., 1975. The elastic energy-momentum tensor. J. Elasticity 5 (3–4), 321–335.

Eshelby, John D., 1999. Energy relations and the energy-momentum tensor in continuum mechanics. In: Fundamental Contributions to the Continuum Theory of Evolving Phase Interfaces in Solids. Springer, pp. 82–119.

Freed, A.D., 2017. A note on stress/strain conjugate pairs: Explicit and implicit theories of thermoelasticity for anisotropic materials. Internat. J. Engrg. Sci. 120, 155–171.

Freed, Alan, Erel, Veysel, Moreno, Michael, 2016. Conjugate stress/strain base pairs for planar analysis of biological tissues. J. Mech. Mater. Struct. 12 (2), 219–247.

Freed, Alan D., le Graverend, Jean-Briac, Rajagopal, K.R., 2019. A decomposition of Laplace stretch with applications in inelasticity. Acta Mech. 230 (9), 3423–3429.

Freed, A.D., Srinivasa, A.R., 2015. Logarithmic strain and its material derivative for a **QR** decomposition of the deformation gradient. Acta Mech. 226 (8), 2645–2670.

Freed, Alan D., Zamani, Shahla, Szabó, László, Clayton, John D, 2020. Laplace stretch: Eulerian and Lagrangian formulations. Z. Angew. Math. Phys. 71 (5), 1–18.

Van der Giessen, Erik, 1989. Continuum models of large deformation plasticity– Part I: Large deformation plasticity and the concept of natural reference state. Eur. J. Mech. A 8, 15.

Van der Giessen, Erik, 1991. Micomechanical and thermodynamic aspects of the plastic spin. Int. J. Plast. 7, 365–386.

Gupta, Anurag, Steigmann, David J., Stölken, James S., 2007. On the evolution of plasticity and incompatibility. Math. Mech. Solids 12 (6), 583–610.

Iwasawa, Kenkichi, 1949. On some types of topological groups. Ann. of Math. 507–558.

Kazerooni, N. Afsar, Srinivasa, A.R., Freed, A.D., 2019. Orthotropic-equivalent strain measures and their application to the elastic response of porcine skin. Mech. Res. Commun. 101, 103404.

Lee, Erastus H., 1969. Elastic-plastic deformation at finite strains. J. Appl. Mech. 36 (1), 1–6.

Lembo, M., 2017. On the determination of deformation from strain. Meccanica 52 (9), 2111–2125.

Lubarda, Vlado A., 2004. Constitutive theories based on the multiplicative decomposition of deformation gradient: Thermoelasticity, elastoplasticity, and biomechanics. Appl. Mech. Rev. 57 (2), 95–108.

Lubliner, Jacob, 2008. Plasticity Theory. Courier Corporation.

Maugin, Gérard A., 2016. Configurational Forces: Thermomechanics, Physics, Mathematics, and Numerics. CRC Press.

McLellan, A.G., 1976. Finite strain coordinates and the stability of solid phases. J. Phys. C: Solid State Phys. 9 (22), 4083.

McLellan, Alister George, 1980. The Classical Thermodynamics of Deformable Materials. Cambridge University Press.

Onsager, Lars, 1931. Reciprocal relations in irreversible processes. I. Phys. Rev. 37 (4), 405.

Paul, Sandipan, Freed, Alan D., 2020a. Characterization of the geometrically necessary dislocations using a Gram–Schmidt factorization of the deformation gradient. Z. Angew. Math. Phys. 71 (6), 196.

Paul, Sandipan, Freed, Alan D., 2020b. A simple representation of the compatibility conditions for a Gram–Schmidt factorization of the deformation gradient. Acta Mech. 231 (8), 3289–3304.

Paul, Sandipan, Freed, Alan D., 2021. A constitutive model for elastic-plastic materials using scalar conjugate stress/strain base pairs. J. Mech. Phys. Solids 155, 104535.

Paul, Sandipan, Freed, Alan D., Benjamin, Chandler C., 2021a. Application of the Gram–Schmidt factorization of the deformation gradient to a cone and plate rheometer. Phys. Fluids 33 (1), 017113.

Paul, Sandipan, Freed, Alan D., Clayton, John D., 2021b. Coordinate indexing: On the use of Lagrangian and Eulerian Laplace stretches. Appl. Eng. Sci. 5, 100029.

Rajagopal, K.R., Srinivasa, A.R., 1998. Mechanics of the inelastic behavior of materials. Part II: Inelastic response. Int. J. Plast. 14 (10–11), 969–995.

Rajagopal, Kumbakonam R., Srinivasa, Arun R., 2004. On thermomechanical restrictions of continua. Proc. R. Soc. Lond. Ser. A Math. Phys. Eng. Sci. 460 (2042), 631–651.

Rajagopal, K.R., Srinivasa, A.R., 2005. On the role of the Eshelby energy-momentum tensor in materials with multiple natural configurations. Math. Mech. Solids 10 (1), 3–24.

Rajagopal, K.R., Srinivasa, A.R., 2016. An implicit three-dimensional model for describing the inelastic response of solids undergoing finite deformation. Z. Angew. Math. Phys. 67 (4), 86.

Rajagopal, K.R., Srinivasa, A.R., 2019. Some remarks and clarifications concerning the restrictions placed on thermodynamic processes. Internat. J. Engrg. Sci. 140, 26–34.
Rodriguez, Edward K., Hoger, Anne, McCulloch, Andrew D., 1994. Stress-dependent finite growth in soft elastic tissues. J. Biomech. 27 (4), 455–467.
Simo, Juan C., Hughes, Thomas J.R., 2006. Computational Inelasticity, Vol. 7. Springer Science & Business Media.
Srinivasa, A.R., 2012. On the use of the upper triangular (or **QR**) decomposition for developing constitutive equations for Green-elastic materials. Internat. J. Engrg. Sci. 60, 1–12.
Zamani, Shahla, Paul, Sandipan, Kotiya, Akhilesh A, Criscione, John C, Freed, Alan D, 2021. Application of QR framework in modeling the constitutive behavior of porcine coronary sinus tissue. Mech. Soft Mater. 3 (1), 1–20.
Zhang, Will, Zakerzadeh, Rana, Zhang, Wenbo, Sacks, Michael S, 2019. A material modeling approach for the effective response of planar soft tissues for efficient computational simulations. J. Mech. Behav. Biomed. Mater. 89, 168–198.
Ziegler, Hans, 1963. Some extremum principles in irreversible thermodynamics, with application to continuum mechanics. Prog. Solid Mech. 4, 93–193.